© 2015. Published by The Company of Biologists Ltd | Journal of Cell Science (2015) 128, 3660-3671 doi:10.1242/jcs.173021

RESEARCH ARTICLE

Polycomb RING1A- and RING1B-dependent histone H2A monoubiquitylation at pericentromeric regions promotes S-phase progression

Mónica Bravo[1], Fabio Nicolini[1], Katarzyna Starowicz[1], Sonia Barroso[2], Carmela Calés[3], Andrés Aguilera[2] and Miguel Vidal[1,*]

ABSTRACT

The functions of polycomb products extend beyond their well-known activity as transcriptional regulators to include genome duplication processes. Polycomb activities during DNA replication and DNA damage repair are unclear, particularly without induced replicative stress. We have used a cellular model of conditionally inactive polycomb E3 ligases (RING1A and RING1B), which monoubiquitylate lysine 119 of histone H2A (H2AK119Ub), to examine DNA replication in unperturbed cells. We identify slow elongation and fork stalling during DNA replication that is associated with the accumulation of mid and late S-phase cells. Signs of replicative stress and colocalisation of double-strand breaks with chromocenters, the sites of coalesced pericentromeric heterocromatic (PCH) domains, were enriched in cells at mid S-phase, the stage at which PCH is replicated. Altered replication was rescued by targeted monoubiquitylation of PCH through methyl-CpG binding domain protein 1. The acute senescence associated with the depletion of RING1 proteins, which is mediated by p21 (also known as CDKN1A) upregulation, could be uncoupled from a response to DNA damage. These findings link cell proliferation and the polycomb proteins RING1A and RING1B to S-phase progression through a specific function in PCH replication.

KEY WORDS: Pericentric heterochromatin, Polycomb, Replication, RING1A, RING1B

INTRODUCTION

Chromatin regulators of the polycomb class are most well-known for their activity repressing developmentally relevant genes (reviewed in Di Croce and Helin, 2013; Lanzuolo and Orlando, 2012; Schuettengruber et al., 2007). Polycomb-dependent silencing relies, at least in part, on histone modifications. Type I and II polycomb repressive complexes (also known as PRC1 and PRC2) monoubiquitylate or methylate specific lysine residues at histones H2A and H3, respectively (Schwartz and Pirrotta, 2013; Simon and Kingston, 2013). These histone modifications are often coupled in a self-reinforcing positive-feedback loop (Kalb et al., 2014a; Klose et al., 2013).

RING1A and its paralogue RING1B (collectively RING1 proteins) are evolutionary conserved RING finger proteins that are present in all E3 ubiquitin ligases of the distinct PRC1 classes. PRC1 E3 ligases are heterodimers made of RING1A or RING1B and a second RING finger protein, out of a six PCGF family members [PCFG4 (also known as BMI1), for example], specific to each PRC1 class (Gao et al., 2012). In this RING-type of E3 ubiquitin ligase, the PCGF subunit acts as a positive cofactor (Buchwald et al., 2006; Cao et al., 2005), whereas the RING1 component binds the E2 ubiquitin-conjugating enzyme and the substrate to which the ubiquitin moiety is transferred (Bentley et al., 2011; Buchwald et al., 2006). Histone H2A monoubiquitylation (H2AK119Ub) positively correlates with gene repression (Endoh et al., 2012; Wang et al., 2004) and it is mostly, but not exclusively, a PRC1-dependent modification. The structure of a monoubiquitylating module (RING1B and BMI1 RING fingers) bound to a nucleosome shows the crucial role of RING1B in histone recognition and positioning of the E2 enzyme for the specific modification of lysine 119 in histone H2A C-terminus (McGinty et al., 2014).

Constitutive inactivation of *Ring1A* in mice is accompanied by developmental alterations compatible with ontogeny and adult life (del Mar Lorente et al., 2000). In contrast, a *Ring1B*-null mutation is embryonic lethal (Voncken et al., 2003). Despite this essential function of RING1B during development, there is ample evidence of functional redundancy between RING1A and RING1B paralogues, for example in embryonic neural stem cells (Román-Trufero et al., 2009) and preimplantation embryos (Posfai et al., 2012). Thus, global H2AK119Ub levels are decreased by the inactivation of either paralogue but are only severely decreased when both are depleted (de Napoles et al., 2004).

Ring1B inactivation leads to phenotypes that combine both differentiation and proliferation defects (Calés et al., 2008; Román-Trufero et al., 2009). The latter are related to upregulation of tumour suppressors that inhibit cyclin-dependent kinases (CDKs) and control cell proliferation by modulating S-phase entry. Some of these inhibitors (CDKIs) are encoded by the *Ink4* (also known as *Cdkn2a* and *Cdkn2b*) locus (Bracken et al., 2007; Calés et al., 2008; Maertens et al., 2010), although their inactivation does not rescue the lethality of *Ring1B*-knockout (KO) embryos (Voncken et al., 2003) suggesting additional RING1B activities during cell cycle progression. One such function could be DNA damage repair (DDR). On irradiated cells, PRC1 subunits migrate to sites of induced DNA damage (Chou et al., 2010; Ginjala et al., 2011) to participate at the earliest signalling and amplification steps of the DDR pathways (Bergink et al., 2006; Lukas et al., 2011; Vissers et al., 2012). Defects in DNA replication have also been observed in double RING1A- and RING1B-deficient two-cell embryos and immortalised fibroblasts (Piunti et al., 2014; Posfai et al., 2012), but

[1]Biología Celular y Molecular, Centro de Investigaciones Biológicas, Consejo Superior de Investigaciones Científicas, Madrid 28040, Spain. [2]Inestabilidad Genómica, Centro Andaluz de Biología Molecular y Medicina Regenerativa (CABIMER), Universidad de Sevilla, Sevilla 41092, Spain. [3]Biología del Cáncer, Instituto de Investigaciones Biomédicas, Consejo Superior de Investigaciones Científicas, Universidad Autónoma de Madrid, Madrid 28029, Spain.

*Author for correspondence (mvidal@cib.csic.es)

Received 13 April 2015; Accepted 12 August 2015

Journal of Cell Science (2015) 128, 3660-3671 doi:10.1242/jcs.173021

the involved processes are poorly characterised. Here, we address the contributions of RING1A and RING1B to DNA replication by immunolocalisation studies in unperturbed cells, shortly after conditional inactivation. The approach overcomes functional redundancy and avoids inducing replication stress, which is associated with oncogene expression (Bartkova et al., 2006; Di Micco et al., 2006) when used to immortalise cultures (Piunti et al., 2014). We found that H2A ubiquitylation at pericentric heterochromatin (PCH) is an essential RING1A- and RING1B-dependent step in cell cycle progression during physiological DNA replication.

RESULTS

RING1A and RING1B depletion results in a rapid p21-dependent proliferative arrest

Proliferation of low passage primary mouse embryonic fibroblasts (MEFs) cultures decreased dramatically soon after addition of 4-hidroxytamoxifen (4′-OHT), a treatment that triggers inactivation of all RING1 activity in *Ring1A*$^{-/-}$, *Ring1B*$^{f/f}$, *Polr2a:Cre-ER*^{T2} cells. Fig. 1A shows a rapid decrease in the frequency of proliferative cells in mutant cultures, as assessed by incorporation of thymidine analogue 5-ethynyl-2′-deoxyuridine (EdU) into DNA compared to in control cells [treated with vehicle, ethanol (EtOH)]. In agreement

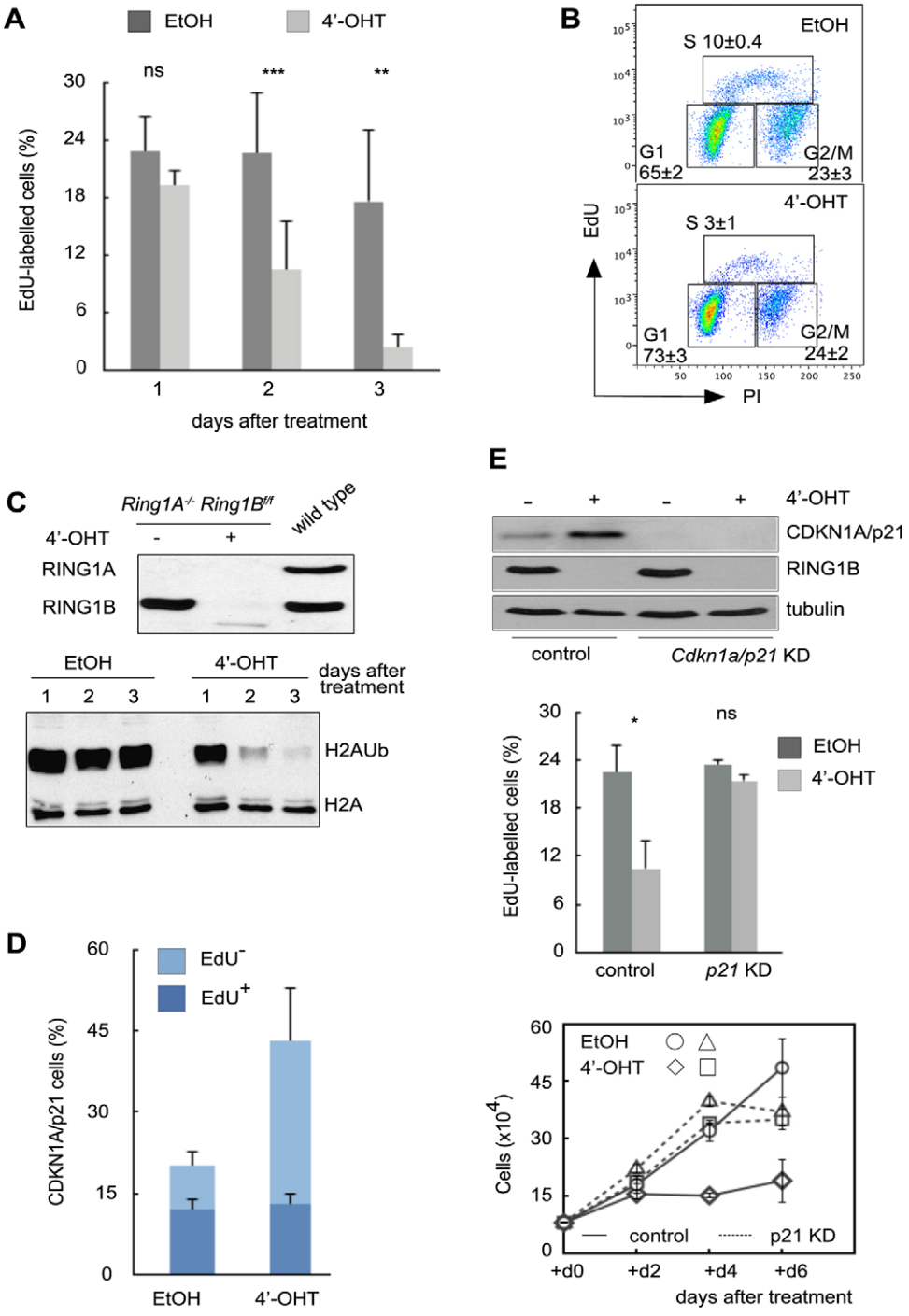

Fig. 1. Acute proliferative arrest of RING1A- and RING1B-deficient cells. (A) Replication, measured as the proportion of cells that incorporated EdU, in *Ring1A*$^{-/-}$, *Ring1B*$^{f/f}$, *Cre-ER* cultures pulsed at the indicated times after treatment with 4′-OHT or EtOH. (B) EdU incorporation and DNA content [propidium iodide (PI)] in cultures 48 h after the indicated treatments showing increased and reduced sizes of mutant cells in G1 and S-phase, respectively. (C) Representative western blots showing RING1A and RING1B and histone content in MEFs of the indicated genotypes and treatments, detected by anti-RING1A, anti-RING1B, anti-H2AK119Ub and anti-H2A (loading control) antibodies. (D) Accumulation of arrested (EdU^{-}) p21 immunolabelled cells (scored in at least 250 cells per condition and experiment) 48 h after the indicated treatments. (E) Top, western blot showing p21 levels in *Ring1A*$^{-/-}$, *Ring1B*$^{f/f}$, *Cre-ER* cells transduced with a lentivirus expressing *p21* shRNA (KD) or control shRNA and treated with EtOH or 4′-OHT; bottom, EdU-labelled cells showing a restored proliferative rate after p21 knockdown. Bar charts show mean±s.d. The number of biological replicates (fibroblast lines derived from independent embryos) was n=8 (A, except 72 h, n=2), n=2 (B,D,E). *$P\leq0.05$; **$P\leq0.01$, ***$P\leq0.004$; ns, not significant ($P\geq0.05$).

Journal of Cell Science (2015) 128, 3660-3671 doi:10.1242/jcs.173021

with this, the numbers of double RING1A- and RING1B-deficient cells hardly increased above those initially seeded (supplementary material Fig. S1A) even though apoptosis, as estimated by caspase-3 immunoreactivity or Annexin V staining, was similar to that in EtOH-treated cultures (supplementary material Fig. S1B). Double EdU and propidium iodide staining allowed the identification, in mutant cultures, of both an enlargement in the G1 and a reduction in the S-phase cell population compared to cultures expressing RING1B (Fig. 1B), indicating a failure in S-phase entry. The timing of decreased proliferation overlapped with that of the depletion of global histone H2AK119Ub levels in 4′-OHT-treated cells (Fig. 1C, bottom).

Proliferative rates of wild-type and *Ring1A*$^{-/-}$ MEFs (supplementary material Fig. S1C) were similar to those of EtOH-treated *Ring1A*$^{-/-}$, *Ring1B*$^{f/f}$, *Polr2a:Cre-ER*^{T2} cells, from now on termed control cells. By contrast, nuclear translocation of Cre-ER protein had no effect on the proliferative rate (supplementary material Fig. S1C), whereas the ectopic expression (through retroviral transduction) of RING1B in mutant MEFs, restored the proportions of EdU-incorporating cells to the values seen in control cells (supplementary material Fig. S1D). Taken together, the data demonstrate that depletion of RING1 proteins is the underlying cause of the rapid proliferative arrest.

RING1A- and RING1B-depleted MEFs upregulated, as expected, the expression of proliferation inhibitors (CDKIs) encoded by the *Ink4a,b* locus (see p16^{Ink4a}, supplementary material Fig. S1E, top). However, the frequency of EdU-incorporating cells in cultures with concurrent inactivation of *Ring1A*, *Ring1B* and *Ink4a,b* was reduced to a similar level to that of mutant cells with an intact *Ink4a,b* locus (supplementary material Fig. S1E, bottom), suggesting that, at least in the short term, proliferative arrest in mutant cells is caused by some other cell cycle regulator. Thus, we tested the CDKI p21, another inhibitor of entry into S-phase and a PRC1 target (Fasano et al., 2007; Román-Trufero et al., 2009). Indeed, Fig. 1D,E shows p21 upregulation, as assessed by western blotting, and an increased number of p21 immunoreactive cells in mutant cultures. In contrast with the inactivation of *Ink4a,b*-encoded CDKIs, short hairpin RNA (shRNA)-mediated downregulation (knockdown) of p21 (Fig. 1E) restored proliferation in RING1A- and RING1B-depleted cells to levels similar to those seen in control cells, thus indicating that proliferative arrest in mutant cells in our model is mediated by p21 upregulation. Cell accumulation tests showed that p21 knockdown rescued the proliferative arrest of RING1A- and RING1B-deficient cells, although only transiently (Fig. 1E).

Fork stalling, replicative stress and double-strand breaks in unperturbed *Ring1A* and *Ring1B* mutant cells

DNA replication was analysed by molecular combing, which allows the examination of individual DNA fibres. We used cultures treated 48 h earlier with 4′-OHT, a time point in our inducible inactivation model in which RING1B and H2AK119Ub levels were very low but where the culture still contained a reasonable fraction of replicating cells. Cultures were pulsed with the thymidine analogues chlorodeoxyuridine (CldU) and iododeoxyuridine (IdU) as indicated in Fig. 2A (top). Analysis of fluorescent signals generated by nucleotide-specific antibodies showed a rather unimodal distribution of elongation speed values in control cultures. Instead, a less homogeneous distribution, in which a larger number of slowly elongating fibres and, conversely, a reduction in the fastest fibres was seen in mutant cultures (Fig. 2A, bottom) resulting in an overall decrease in fork progression. In order to investigate whether the slow elongation might have resulted from DNA polymerases stalling, we then measured differences in track lengths on one or both directions from a common origin (uni- or bi-directional, respectively), which is indicative of fork stalling. Our results showed that fibres prepared from mutant cultures contained a larger proportion of asymmetric signals of either pattern than those from control cells (Fig. 2A, right), consistent with an augmented frequency of fork-stalling events.

Further evidence for stalled replication was obtained by looking at replication protein A (RPA), which binds and protects single-stranded DNA generated at sites of replicative stress (Zou and Elledge, 2003). To detect insoluble replication-associated RPA we extracted EdU-pulsed cultures with detergent, prior to fixation. Scoring double EdU^{+} and RPA32^{+} (RPA32 is also known as RPA2) cells, we found almost a twofold increase in replicative stress among mutant cultures (25.8±5.2% versus 14.2±4.1%, mean±s.d., Fig. 2B; examples of EdU^{+} and RPA32^{-} cells are shown in supplementary material Fig. S2A). In addition, double-strand break (DSB) markers, such as phosphorylated histone γH2AX (S139) and the tumour suppressor p53-binding protein 1 [53BP1 (Balajee and Geard, 2004; Wang et al., 2002)] were preferentially enriched among mutant cells undergoing replicative stress (Fig. 2C). Collectively, these results show fork stalling and replicative stress in unperturbed cells lacking RING1A and RING1B.

Defective replication at PCH in RING1A- and RING1B-defective cells

We exploited the fact that MEFs show cytologically defined S-phase stages that are easily distinguished by characteristic spatio-temporal patterns of DNA synthesis (Quivy et al., 2004; Wu et al., 2006) to determine whether altered replication in RING1A- and RING1B-deficient cells affected such patterns. We used asynchronous MEF cultures, 48 h after EtOH or 4′-OHT treatment, and pulsed them with IdU for 20 min in order to score the proportion of cells in each of the S-phase stages. The results clearly showed that mutant cultures contained larger proportions of mid and late S-phase cells compared to controls (Fig. 3A).

We then reasoned that the slowed or stalled replication seen above could be the underlying cause of such abnormal frequencies of mid and late S-phase mutant cells. We carried out a kinetic assay that used a double pulse and chase labelling in which cultures received a short EdU pulse, and after an hour, an IdU pulse (Fig. 3B, left). The S-phase stage was scored using EdU staining and then, incorporation of IdU was used to define three patterns corresponding to transitions between S-phase stages (Fig. 3B). In pattern I, cells showed both early EdU and middle IdU signals. Type II cells showed middle EdU and late IdU signals. Finally, in type III, incorporation of only EdU indicated completion of S-phase during the chase period. Differences in the relative proportions of these patterns could then be interpreted as progression through S-phase at a distinct speed. The proportion of cells displaying pattern I (cells progressing from early into middle S-phase) was similar between both cultures (36.2±1.6% versus 33.5±4.1%, mean±s.d., for control and mutant, respectively). In contrast, transitions from middle or late S-phase (patterns II and III) were under-represented in mutant cultures (52.1±6.8% vs 85.0±3.5% and 47.7±3.1 versus 92.3±7.1%, respectively; bar charts in Fig. 3B, right), suggesting that the progression of mutant cells through mid and late S-phase, occurred slower than in control cells. In fact, the extent of colocalisation of IdU and EdU signals per cell was lower in control than in mutant cultures (Fig. 3C), in agreement with replication occurring in a more dynamic fashion in RING1B-expressing cells. To determine whether RING1A expression alone would rescue the replication defects we used *Ring1B*$^{f/f}$, *Polr2a:Cre-ER*^{T2} cells. Upon 4′-OHT-

Journal of Cell Science (2015) 128, 3660-3671 doi:10.1242/jcs.173021

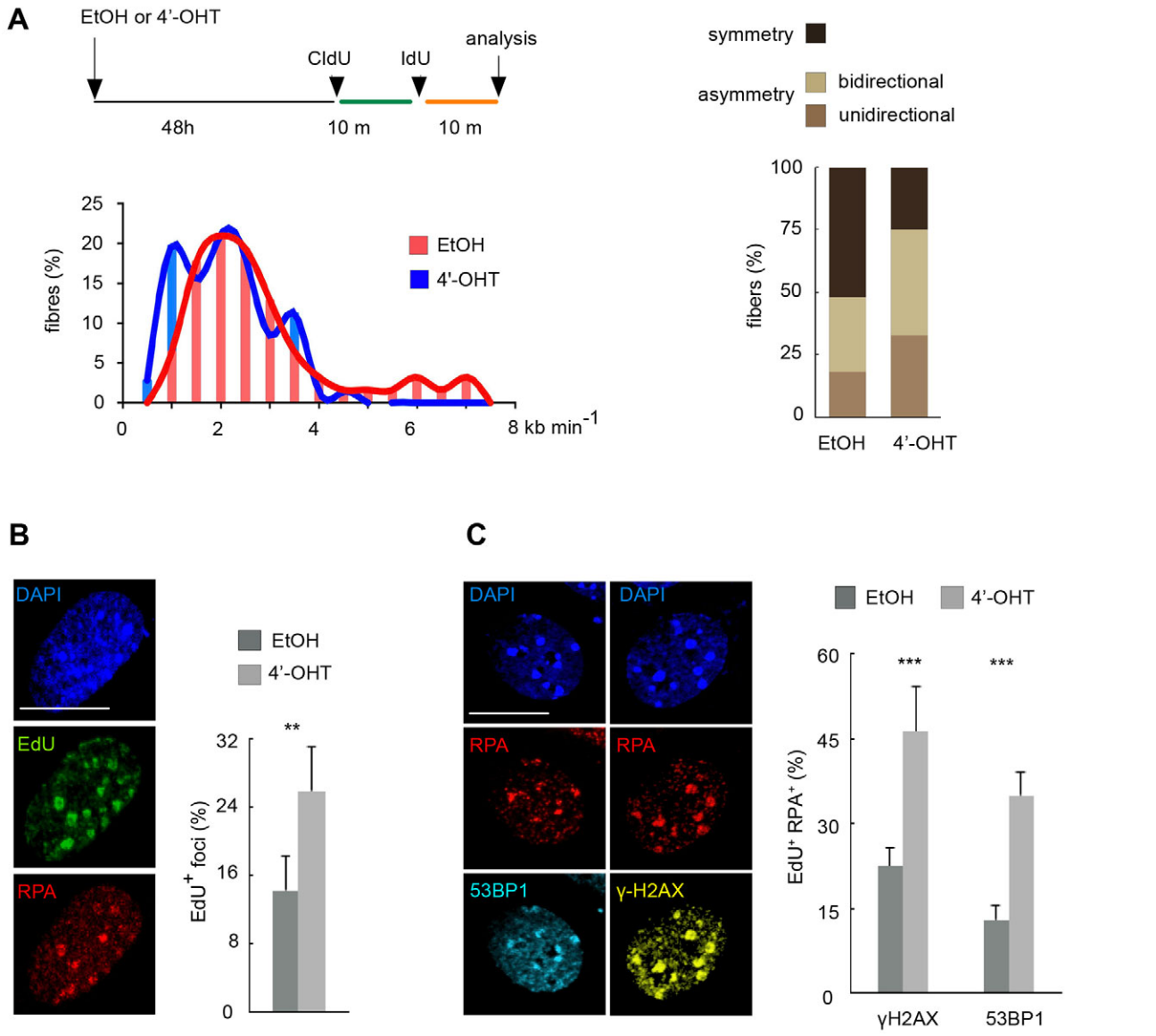

Fig. 2. Defective DNA replication and DNA damage in unperturbed RING1A- and RING1B-depleted cells. (A) Top left, schematic of the pulse experiment with thymidine analogues for DNA fibre analysis; bottom, distribution of progression speed in single DNA fibres in mutant (treated with 4′-OTH) and control (treated with EtOH) cultures. At least 150 fibres were counted for each condition in three independent experiments. The bar charts (right) show the proportions of fibres replicating symmetrically (with equal length bidirectional tracks) or asymmetrically, with uni- and bi-directional tracks. At least 80 fibres were scored for each condition in two independent experiments. (B) Replicative stress assessed by immunodetection of chromatin-bound RPA32 (left) showing an increased frequency of double EdU^+, RPA^+ cells in mutant cultures. (C) Increased DSBs in replicative cells indicated by cells showing γH2AX, 53BP1 and RPA labelling (left); bar charts display the frequencies of triply labelled cells among, at least, 100 EdU^+ and RPA^+ doubly stained cells. Bar charts are mean±s.d. The number of independent experiments was n=4 (B), n=3 (C). $^{**}P$=0.01; $^{***}P \leq 0.003$; ns, not significant ($P \geq 0.05$). Scale bars: 10 µm.

induced RING1B depletion, we found that, in the presence of RING1A, both transition patterns and S-phase stage distributions were as in control cells (supplementary material Fig. S2C), demonstrating functional equivalence between the two paralogues during replication.

It is known that MEFs replicate PCH during mid S-phase, and centromeric heterochromatin at late S-phase (Guenatri et al., 2004). Indeed, we found colocalisation of replication (IdU signals) and histone H3 trimethylated at lysine 9 (H3K9me3) foci, characteristic of PCH (Guenatri et al., 2004), in mid-S-phase cells, but not in early or late S-phase cells in both control and mutant cultures (supplementary material Fig. S2B, top left). Interestingly, the extent of colocalised IdU–H3K9me3 signals in mutant cells was significantly lower than in controls, as would be expected if IdU incorporation at PCH was reduced (supplementary material Fig. S2B, top right). Therefore, we anticipated that replicative stress in RING1A- and RING1B-deficient cells would also accumulate at mid-late S-phase. To test this hypothesis, we assessed the distribution of replicating (EdU^+) cells with RPA foci with respect to S-phase stages. The results showed a much larger enrichment of RPA immunoreactivity among mutant mid and late S-phase cells than in controls (59.3±7.5% versus 28.3±3.5% for mid S-phase; 33.3±5.8% versus 14.0±2.64% for late S-phase), frequently colocalising with H3K9me3 foci (Fig. 3D, left; examples of $H3K9me3^+$ and RPA^- cells are shown in supplementary material Fig. S2B, bottom right). Given that H3K9me3 and 4′,6-diamidino-

Journal of Cell Science (2015) 128, 3660-3671 doi:10.1242/jcs.173021

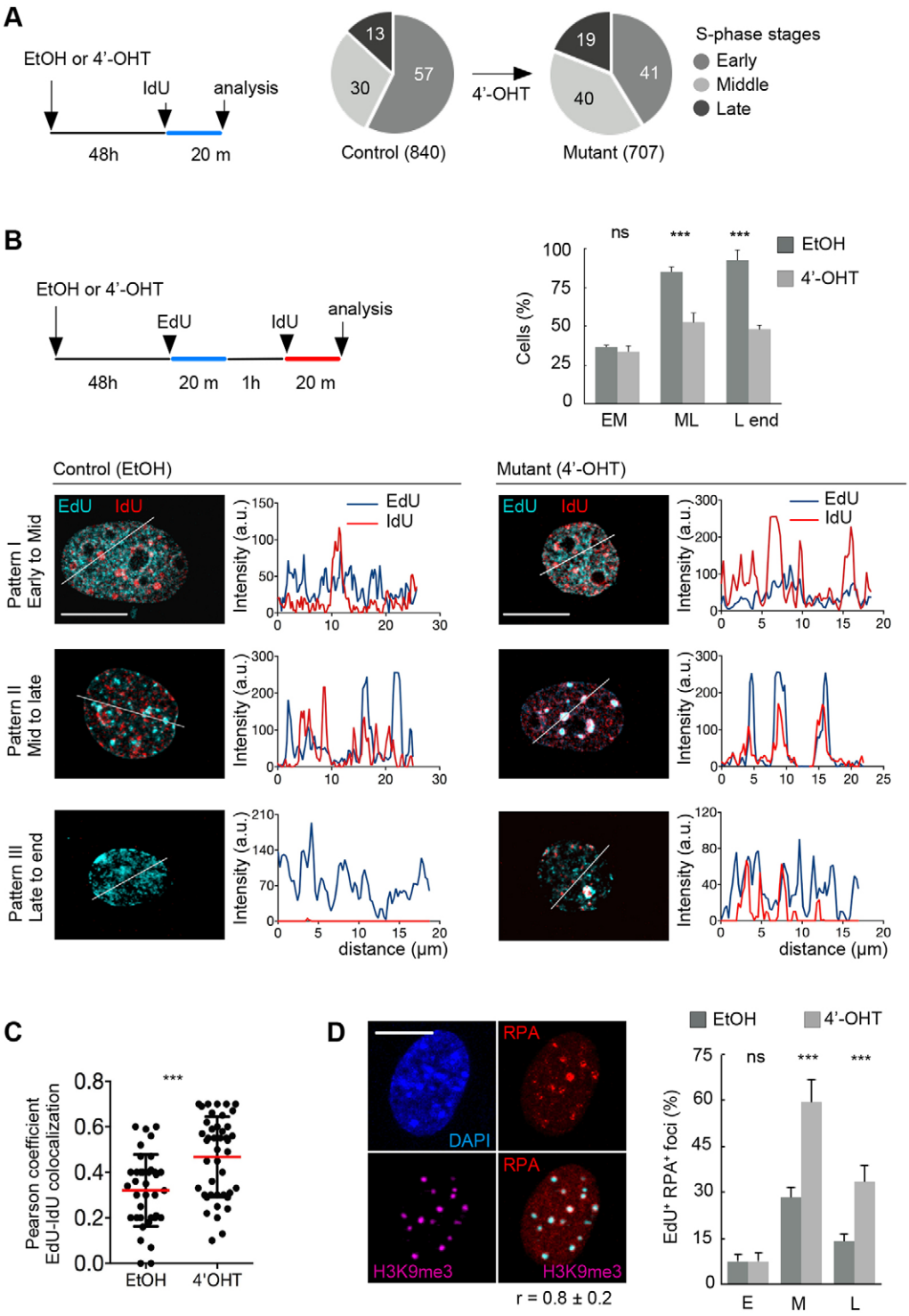

Fig. 3. Defective S-phase progression during replication of PCH. (A) Pie charts showing the proportions of cells in each stage of S-phase scored after the indicated IdU pulse. Labelled cells, in randomly selected fields, were counted (total number between brackets) until at least 50 cells were scored for the least frequent stage (late S-phase) in four independent experiments. (B) Transitions through S-phase stages. Top left, schematic of the labelling protocol. Top right, relative frequencies of the indicated transition patterns in control and mutant cultures; values show the mean±s.d. frequency from at least 50 cells per phase stage (determined at the EdU pulse) in each of three independent experiments cells. EM, ML and L end, represent early-mid, mid-late and late-to-end S-phase stages, respectively. Bottom left, representative EdU and IdU staining in control cultures showing patterns defining the indicated transition patterns. Bottom right, examples of cells with impaired transitions in mutant cultures. Bar charts are intensity profiles of immunostaining across the nucleus of representative cells at the position indicated by the line. (C) Colocalisation of EdU and IdU signals in cultures pulsed as in A. (D) Augmented frequency of mutant cells showing replicative stress at PCH. Left, representative immunofluorescence images of a mid-S-phase mutant cell showing (partial) colocalisation of RPA and the PCH marker H3K9me3; the Pearson coefficient, r, for RPA–H3K9me3 signal colocalisation (at least 50 double-positive cells in each of two experiments) is shown. Right, distribution of RPA-immunoreactive cells in each of S-phase stages. E, M and L represent early, mid and late S-phase stages, respectively. Data are mean±s.d.; n=3 (C,D). ***$P \leq 0.006$; ns, not significant ($P \geq 0.05$). Scale bars: 10 μm.

2-phenylindole (DAPI) patterns were similar in control and mutant cultures (supplementary material Fig. S2B, bottom left), effects on global chromatin structure secondary to RING1A and RING1B depletion appeared unlikely. Taken together, the data link RING1A and RING1B to the replication of pericentromeric domains.

RING1A and RING1B H2A monoubiquitin ligase activity is required for PCH replication

RING1B involvement in gene repression occurs through mechanisms dependent and independent of its ubiquitin ligase activity (Eskeland et al., 2010; Isono et al., 2013). We asked whether defective replication correlated with histone H2AK119Ub at major satellite chromatin (i.e. large arrays of tandem copies of 234 bp segments, the major constituent of PCH, Fig. 4A) (Guenatri et al., 2004). Chromatin immunoprecipitation (ChIP) in control cells showed H2AK119Ub enrichment at these domains, but it was wiped out in mutant cells after only 48 h of treatment, in agreement with the highly dynamic turnover of this histone mark (Alchanati et al., 2009). In addition, we also found RING1B occupying major satellites in control cells (Fig. 4B). Of

Journal of Cell Science (2015) 128, 3660-3671 doi:10.1242/jcs.173021

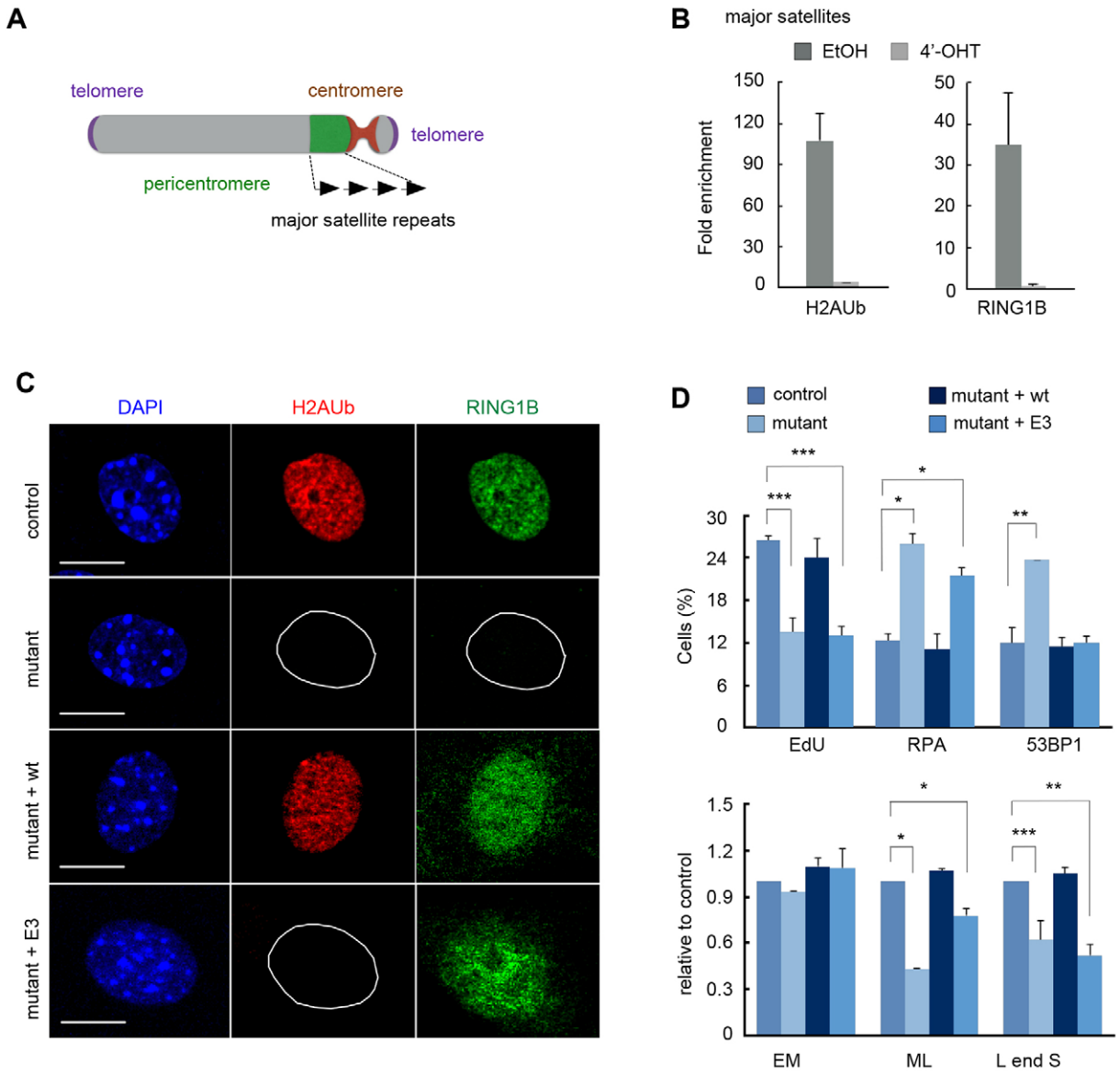

Fig. 4. Delayed mid- and late-S-phase progression correlates with loss of RING1B-dependent monoubiquitylation of pericentric histone H2A. (A) Cartoon depicting constitutive heterochromatic domains and the location of major satellite repeats at pericentric regions. (B) Histone H2AK119Ub enrichment and RING1B occupancy at PCH. Data are mean±s.d. from three independent ChIP experiments. (C) Representative cells of *Ring1A*$^{-/-}$, *Ring1B*$^{f/f}$, *Cre-ER* cultures treated with EtOH (control) or 4′-OHT (mutant); cultures were transduced with retrovirus that expressed wild-type RING1B (mutant+wt) and E3-inert RING1B (mutant+ΔE3); endogenous (control) and ectopic RING1B was detected with anti-RING1B and anti-FLAG antibodies, respectively, whereas the modified histone H2A was detected with anti-H2AK119Ub antibody. In the absence of immunofluorescent signals, nuclei boundaries are marked by a white mask generated from the DAPI channel for the same cell. (D) Top, summary of the proliferative rate (EdU incorporation), replicative stress (RPA) and DSBs (53BP1 foci) for the indicated cultures. Values are percentage of total cells in the culture (EdU, 1 h pulse) and of the replicative fractions (EdU^{+}) that also are immunoreactive for RPA or 53BP1. Bottom, S-phase progression in the indicated cultures assessed as in Fig. 3B; ratios were calculated using those of control cells as a reference. EM, ML and L end S, represent early-mid, mid-late and late-to-end S-phase stages, respectively. Data are mean±s.d.; n=3 (B,C and D, top), n=2 (D, bottom). *P=0.01–0.04; ***P≤0.007. Scale bars: 10 µm.

note, the absence of RING1B or H2AK119Ub on major satellites had a negligible effect on the PRC2-dependent modification of histone H3K27me3 (supplementary material Fig. S3A).

Given the known correlation between H2AK119Ub and gene repression, we tested the possibility of derepression of major satellites as a source of defective replication associated with interference in ongoing transcription (Helmrich et al., 2013). We measured the level of major satellite transcript by quantitative real-time PCR (qRT-PCR) (supplementary material Fig. S3B) and found no significant differences between control and mutant cells, thus ruling out a possible source of replicative stress at PCH.

Given that the compound depletion of RING1 proteins induces E3-ligase-dependent and -independent effects, we decided to test a RING1B variant, termed ΔE3, that carries an I53A,L55A mutation and therefore is only deficient as a ubiquitin ligase (Buchwald et al., 2006; Endoh et al., 2012). Whereas control and wild-type RING1B-transduced cells readily showed histone H2AK119Ub labelling, cell cultures transduced with RING1B ΔE3 lacked H2AK119Ub, as in RING1A- and RING1B-depleted cells (Fig. 4C). A more sensitive

Journal of Cell Science (2015) 128, 3660-3671 doi:10.1242/jcs.173021

analysis (ChIP) showed no H2AK119Ub enrichment at major satellites of RING1B-ΔE3-transduced cells, despite occupancy by the RING1B variant (supplementary material Fig. S3C,D). A kinetic analysis of replication progression through S-phase stages, using double pulse and chase experiments, as above, showed that, although ectopic intact RING1B rescued the delayed replication at PCH, cells that expressed the E3 variant showed decreased frequencies of transitions through mid to late S-phase and late S-phase patterns corresponding to the delayed replication at these stages seen in RING1A- and RING1B-deficient cells (Fig. 4D). Likewise, proliferation (EdU incorporation) and replicative stress levels (RPA foci) in RING1B-ΔE3-expressing cultures were also similar to those seen in the double mutant cells (Fig. 4D). Taken together, the results show that E3-dependent functions are essential for PCH replication, although a H2A–ubiquitin ligase-independent activity can be inferred from the normal frequency of DSB signals (EdU^+ and $53BP1^+$) seen in RING1B-ΔE3-transduced cells (Fig. 4D).

Targeted monoubiquitylation of PCH histone H2A rescues DNA replication of RING1A- and RING1B-deficient cells

To test the notion that RING1A- and RING1B-dependent monoubiquitylation of histone H2A underlies the altered replication seen in RING1-deficient cells, we used a ubiquitylating module made of linked RING fingers from RING1B and BMI1 (Cooper et al., 2014) that mimics the heterodimeric E3 ligase for histone H2A (Buchwald et al., 2006). Targeting to PCH was achieved through the DNA-binding domain of methyl-CpG binding domain protein 1 (MBD1) which associates with the enriched methyl-CpG sites found at major satellites (Cooper et al., 2014). Expression of MBD1–RING1B–BMI1 (MBD1-RB, Fig. 5A) protein resulted in nuclei with strong H2AK119Ub signals at DAPI-labelled chromocentres (Fig. 5B). When the cells were treated with 4′-OHT the pannuclear H2AK119Ub signal (generated by endogenous RING1B) was lost, remaining only at chromocentres, thus showing specific targeting of the ubiquitylating module to PCH. Moreover, H2AK119Ub enrichment at regulatory regions of *p21* in control cells, which is lost after RING1A and RING1B depletion, was not restored upon expression of MBD1-RB (supplementary material Fig. S4B), in agreement with preferential targeting of ubiquitylation to MBD1 recognition sites at PCH. Additionally, we confirmed that H2AK119Ub signals in RING1A- and RING1B-deficient cells were strictly dependent on the ability of RING1B–BMI1 module to interact with E2 ligase, because a similarly targeted fusion protein with inactivating mutations (I53A and C51G in the RING1B and BMI1 ring fingers, respectively, MBD1-RBΔE3) produced no H2AK119Ub signal (supplementary material Fig. S4A).

Examination of DNA replication showed that MBD1-RB-expressing cells, despite lacking RING1A and RING1B, progressed through mid-late S-phase stages with similar kinetics to those in control cultures (Fig. 5C, left). Thus, by targeting H2AK119Ub to PCH, the defective replication associated with RING1A and RING1B depletion was corrected. As anticipated, MBD1-RBΔE3, failed to restore normal replication (Fig. 5C, left). The frequencies of cells showing signals of replicative stress (RPA foci) or DSB (53BP1 foci) were similar to that of control cells (Fig. 5C, right), as would be expected if replication is unaltered. This further supported rescue of the replication phenotype. In contrast, MBD1-RB-expressing cells still showed proliferative arrest (as a decreased proportion of EdU^+ cells), consistent with upregulated p21 (Fig. 5C, right) and with the inability of MBD-RB to restore H2AK119Ub onto *p21* regions (supplementary material Fig. S4B). Note that CDKI-dependent arrest of entry to S-phase in mutant cells is not necessarily related to DNA damage responses and, instead is rather a consequence of p21 upregulation. Finally, the increased proportion of mid and late S-phase RING1A- and RING1B-deficient cells returned to control values upon expression of MBD1-RB, additionally supporting the hypothesis that PCH histone H2AK119Ub is required for replication.

DISCUSSION

Our observations imply a functionally relevant involvement of RING1A and RING1B in normal DNA replication. By using unperturbed primary cells our results are not affected by possible confounding effects due to exogenous replicative stress induced by oncogenic overexpression (Bartkova et al., 2006; Di Micco et al., 2006), which was used to immortalise of RING1A- and RING1B-deficient cells in a previous report (Piunti et al., 2014). We also identify monoubiquitylation of histone H2A at major satellites in PCH as an essential event during replication.

RING1A and RING1B function during PCH replication

In unperturbed RING1A- and RING1B-deficient cells, we have detected a subset of replication forks that, compared to control cells, either elongate more slowly or are stalled. The effect was similar to that reported for immortalised *Ring1A* and *Ring1B* mutant cells, although somewhat weaker, possibly due to the previous overexpression of SV40 large T antigen and/or H-RasV217 oncogenes (Piunti et al., 2014). Furthermore, our cytological analysis identified these pausing cells, with signs of replicative stress, among the mid (and also late) S-phase population, showing that DNA replication is particularly sensitive to RING1A and RING1B at the time of PCH duplication.

The presence of RING1B on nascent DNA and, the presence of RING1A on the maturing chromatin following the formation of nascent DNA (Lee et al., 2014; Piunti et al., 2014; Alabert and Groth, 2012), suggests that RING1 proteins have a role in DNA replication. It is now established that, together with other polycomb products, a large cohort of chromatin modifiers is in close proximity with the core replicating machinery of helicases, polymerases and fork stabilisers (Alabert et al., 2014; Petruk et al., 2013). Some of these modifiers, like RING1A and RING1B, are also involved in heterochromatin replication. Examples of such factors include ubiquitin-like with PHD and ring finger domains 1 (UHRF1), an E3 ubiquitin ligase required for the maintenance of DNA methylation (Nishiyama et al., 2013; Papait et al., 2007), and the p150 subunit (CHAF1A) of chromatin-associated factor 1 (CAF1) (Quivy et al., 2008), as well as subunits of chromatin remodellers, such as ATP-utilising chromatin assembly and remodelling factor 1 (ACF1) (Collins et al., 2002) and the CHD4 and MBD3 subunits of the NuRD complex (Sims and Wade, 2011). Loss-of-function mutations in these genes lead, however, to accumulation of cells in early S-phase, rather than the mid to late S-phase that we see in RING1A and RING1B mutant cells. Moreover, the defects in heterochromatin structure seen in some of these mutants (Sims and Wade, 2011) are not observed in RING1A- and RING1B-depleted cells. The differences might relate to the mechanisms by which either of these chromatin regulators participate in PCH replication. The distinctive accumulation of RING1 mutant cells during mid S-phase probably points at an altered replication function intrinsic to these genomic regions. For instance, in the resolution of spontaneous fork stalling at sites that are difficult to replicate, like repetitive sequences (Branzei and Foiani, 2010; Buonomo et al.,

Journal of Cell Science (2015) 128, 3660-3671 doi:10.1242/jcs.173021

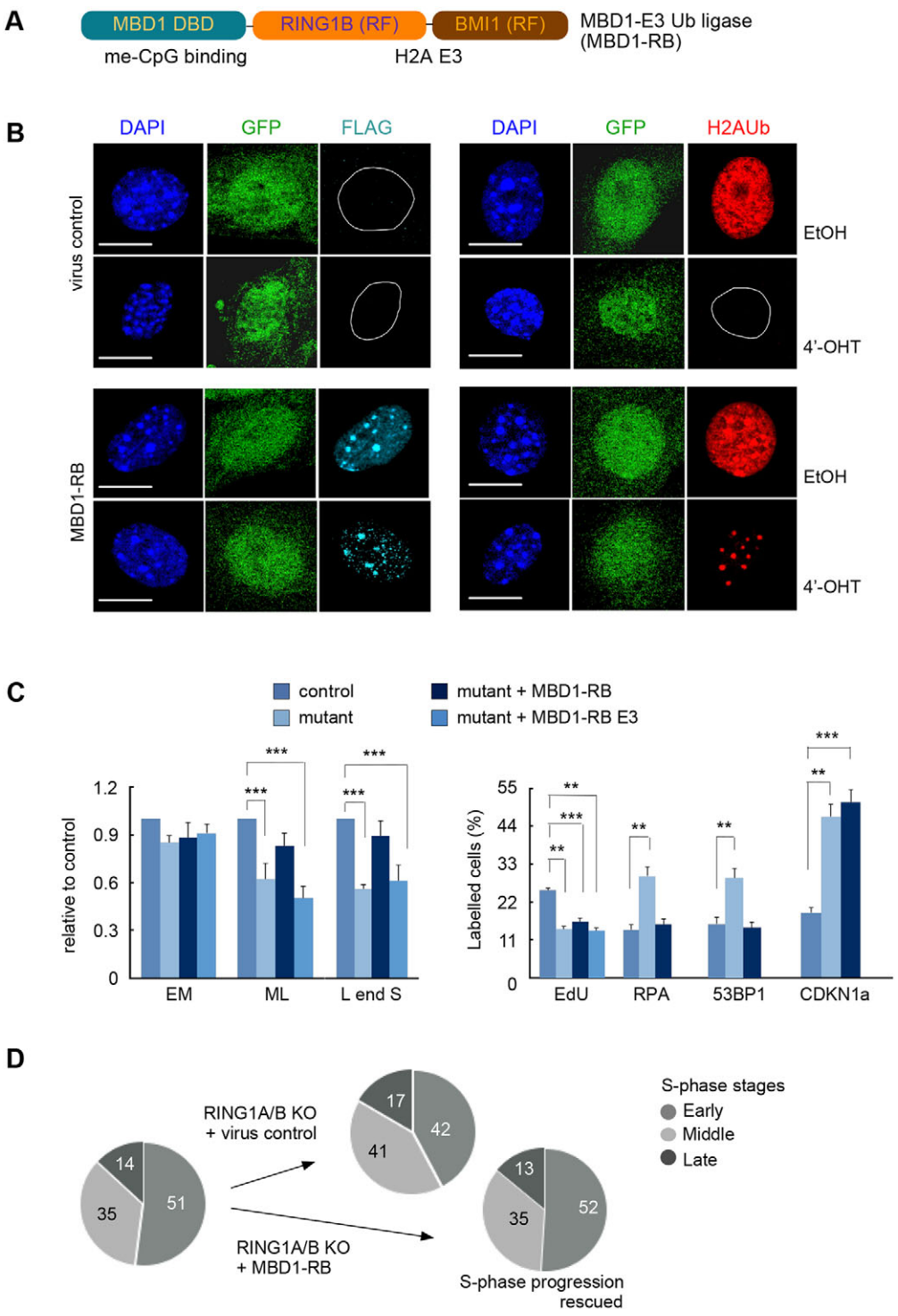

Fig. 5. Targeting RING1B-dependent H2AK119 monoubiquitylation to PCH rescues S-phase progression. (A) Cartoon depicting the fusion protein used to target a histone H2A monoubiquitylating module [RING1, BMI1 RING fingers (RF)] to PCH through the methyl-CpG binding domain of MBD1. (B) Complementation assays upon retroviral transduction of MBD1-RB or empty (control) viruses. Pan-nuclear H2AK119Ub (H2AUb) signals are seen in cells expressing endogenous RING1B, and speckled signals on chromocenters in MBD1-RB-transduced cells lacking RING1A and RING1B. GFP and FLAG mark transduced cells and expression of MBD1, respectively. In the absence of immunofluorescent signals, nuclei boundaries marked by a white mask generated from the DAPI channel for the same cell. (C) Left, S-phase progression in the indicated cultures. MBD1-RBΔE3 is a variant fusion protein lacking ubiquitin E3 ligase activity. Transitions between stages as indicated in Fig. 3; values are normalised to those in control (EtOH-treated) cells. EM, ML and L end S, represent early-mid, mid-late and late-to-end S-phase stages, respectively. Right, proportion of cells within the indicated cultures scored positive for EdU (proliferative rate), RPA and 53BP1 (DNA damage) and p21 (CDKN1a, proliferative arrest). Values are the percentage of total cells [EdU (1 h pulse) and p21)] or the fraction of replicative cells (EdU^+) that are immunoreactive for RPA or 53BP1. (D) Pie charts showing distribution of replicating cells within S-phase stages in cultures pulsed with IdU for 20 min pulse after the indicated treatments. Ectopic MBD1-RB rescued the delayed progress through S-phase of RING1A- and RING1B-depleted (KO) cells. Data are mean±s.d.; n=3 (C,D). $^{**}P$=0.003; $^{***}P \leq 0.0004$. Scale bars, 10 µm.

2009). This proposition seems inconsistent with a general role that might be deduced from the decreased association of histones and proliferating cell nuclear antigen (PCNA, a DNA clamp acting as a processivity factor for polymerases) on replication forks in knocked down RING1B tissue culture cells (Lee et al., 2014). Nonetheless, such a type of widespread activity throughout S-phase would not explain the PCH-specific defects we see in RING1A- and RING1B-deficient cells. In this regard, we think that H2A modification at PCH might be achieved without stable residence of large amounts of RING1B, likely required for immunolocalisation or proteomic analysis, but through rather transient association, given that histone modification detected by ChIP reads catalytic activity.

Replicative stress at PCH, and the RING1A- and RING1B-dependent H2AK119Ub modification

We have shown that targeting histone monoubiquitylation to PCH nucleosomes suffices to rescue defective replication. Replicative stress associated with RING1A and RING1B inactivation, or the expression of an inert E3 ubiquitin ligase RING1B variant, co-occurs with a generalised loss of H2AK119Ub. Possibly, this relates

Journal of Cell Science (2015) 128, 3660-3671 doi:10.1242/jcs.173021

to the partial colocalisation of H2AK119Ub and PCNA signals previously reported in late S-phase (Vassilev et al., 1995). The requirement for histone H2A monoubiquitylation during S-phase at some chromosomal domains and not at others implies a partitioning of the genome, and extends the functionality, directly or indirectly, of this modification beyond control of transcription.

Unscheduled transcription of major satellite repeats, triggered by the lack of H2AK119Ub, seemed a possible source of replicative stress, as a hypothetical upregulation of transcriptional activity, which in mouse cells is normally highest at the G1/S transition and early S-phase (Lu and Gilbert, 2007), might have interfered with PCH replication in mid S-phase. In fact, derepression of major satellite transcripts has been associated with H2AK119Ub loss in cells lacking the E3 ligase BRCA1 (Zhu et al., 2011). However, recent work has shown that it is lysine 127 and lysine 129 of H2A, and not lysine 119, the actual substrate of BRCA1, that mediate this effect (Kalb et al., 2014b). Besides, no upregulation of major satellite transcripts has been detected in single *Ring1B* mutant cells (Zhu et al., 2011). By contrast, H2AK119Ub having little influence on transcriptional silencing at PCH is consistent with its repression being mediated mostly through mechanisms involving methylation of histone H3K9 and DNA (Bulut-Karslioglu et al., 2012; Sharif et al., 2007). Furthermore, it is known that cells undergoing derepression off major satellite repeats show few proliferative alterations and a small DNA damage response (Bulut-Karslioglu et al., 2012). Therefore, we rule out the possibility that PCH replicative stress in RING1A- and RING1B-deficient cells relates to replication interference caused by derepression of major satellites.

RING1B-dependent monoubiquitylation of histone H2A has also been involved in recruiting INO80, the ATPase common to the family of SWI/SNF remodellers, to replication forks (Lee et al., 2014). INO80 activity in DNA replication, however, seems to be rather general, meaning it is unlikely to mediate a PCH-specific replication defect. A more-appealing candidate is S-phase-stage-specific deposition of histone H2A, as has been recently discovered (Boyarchuk et al., 2014). Nucleosomal density during replication is maintained by recycling of parental histones together with the incorporation of newly synthesised histones, and the efficiency of this process influences fork progression (Groth et al., 2007; Jasencakova et al., 2010; Mejlvang et al., 2014). Of note is that, whereas in euchromatin the deposition of newly synthesised histone H2A occurs throughout the cell cycle, at PCH it is a strictly replication-dependent process (Boyarchuk et al., 2014). Perhaps, this temporally restricted deposition of H2A at PCH is linked to nucleosomal reconstitution and chromatin maturation processes accompanying transient structural changes at the periphery of PCH domains where DNA replication actually takes place (Quivy et al., 2004). In the light of our results, assessing the effect of H2A modification on deposition of newly synthesised H2A onto replicating PCH merits investigation.

An H2AK119Ub-independent role of RING1 proteins in replication?

Unperturbed, proliferating cells lacking RING1A and RING1B frequently develop DSBs, possibly as the outcome of defective repair at sites of replicative stress. This was also observed in immortalised cells (Piunti et al., 2014). This could result, at least in part, because of the reported requirement for PRC1-dependent monoubiquitylation of histones H2A and γH2AX at the early stages of repair of induced DSBs (Ginjala et al., 2011; Ismail et al., 2010; Pan et al., 2011; Wu et al., 2011). However, our observation that the frequency of DSBs in cells expressing RING1B ΔE3 is similar to that of control cells, despite the replicative stress, points at RING1B functions in DNA repair independent of its E3 ligase activity. It is possible that this H2AK119Ub-independent activity is difficult to distinguish in DSB studies that use irradiated cells, because this involves preforming DSBs in all stages of the cycle. Thus, H2A-modification-dependent and -independent functions of RING1B in DNA replication and repair are reminiscent of RING1B transcriptional repression mediated by H2A ubiquitylation and chromatin compaction (Eskeland et al., 2010). If a similar structural role were to be at action in hypothetical DNA damage repair situations, perhaps assisting in the recruiting of machinery involved in the stabilisation and/or resolution of stalled forks (Cimprich and Cortez, 2008; Lambert and Carr, 2013), it would be expected that it would be rather local or activated in response to stress, given that neither RING1B nor other PRC1 subunits is found among the constitutive components of PCH (Saksouk et al., 2014). The implications are that under physiological stress, before the formation of DSBs, RING1 proteins, independently of their ability to monoubiquitylate H2A, might play an unanticipated role in genome stability.

In summary, RING1 paralogues control the cell cycle in G1 by indirect modulation of CDKs and repairing damaged DNA but also promote PCH replication through both H2AK119Ub-dependent and -independent mechanisms.

MATERIALS AND METHODS

Tissue culture and cell treatments

Mouse embryonic fibroblasts (MEFs, passage +2) were established from *Ring1A*$^{-/-}$, *Ring1B*$^{f/f}$, *Polr2a:Cre-ER*^{T2} 13.5 dpc embryos (Román-Trufero et al., 2009). For experiments using CDKN2A and CDKN2B-deficient MEFs, the above mouse strain was mated to *Ink4a,b*$^{-/-}$ mice (Krimpenfort et al., 2007). MEFs were grown in Dulbecco's modified Eagle's medium (DMEM; Invitrogen, Life Technologies) supplemented with 10% fetal bovine serum (FBS, Sigma-Aldrich) and antibiotics (Pen-Strep, Life Technologies) in a 5% CO_2 atmosphere. Cells (10^5) were seeded on p60 dishes (Falcon, Becton Dickinson) and, the next day, 4′-OHT (1 µM, Sigma-Aldrich) was added to the culture for 16 h. Analysis was performed at 48 h after treatment initiation, or at the indicated times. 293 T cells were maintained in DMEM with 10% FBS and antibiotics. For cell accumulation assays, cells (seeded in duplicate dishes) were harvested and counted every 2 days.

Retroviral particles were obtained upon transfection of Platinum-E 293 T packaging cells with pMSCV-based plasmids. Briefly, 3×10^6 cells per 10-cm dish received 10 µg plasmid DNA complexed with Turbofect transfection reagent. FLAG-tagged wild-type and mutant RING1B cDNAs were generated by PCR. The RING1B E3 variant (I53A,L55A) cDNA was generated by site-directed mutation using overlap extension PCR. MBD1-RB cDNAs were as described previously (Cooper et al., 2014). For lentiviral particles, 7.5 µg pFUGW-H1 plasmids (Fasano et al., 2007) were co-transfected into 293 T cells with 4.8 µg psPAX2 packaging and 2.6 µg pMD2G envelope plasmids [psPAX2 and pMD2G were gifts from Didier Trono (Addgene plasmids# 12260 and 1259, respectively)]. Viral particles were harvested 48 and 72 h after transfection, filtered through 0.45 µm PVDF membrane filters, aliquoted and stored at −80°C.

Transductions (1×10^5 cells on 6-cm dishes with coverslips) were performed by incubating cells with supernatants containing viral particles and 4 µg/ml polybrene (Sigma-Aldrich) for 16 h. Then, fresh medium was added and, the following day, infected cells were selected by incubating for 48 h in medium containing puromycin 1.1 µg/ml. After 2 days, puromycin medium was removed and cells were treated with EtOH or 4′-OHT.

Immunofluorescence and image processing

Cells grown on glass coverslips were fixed in 4% paraformaldehyde (PFA, Pierce) for 15 min, permeabilised with 0.5% Triton X-100 in Tween-20-containing phosphate-buffered saline (TPBS), and blocked for 30 min in

Journal of Cell Science (2015) 128, 3660-3671 doi:10.1242/jcs.173021

TPBS containing 1% gelatin from cold water fish skin (Sigma-Aldrich) and 10% goat serum (blocking buffer). For analysis of replication proteins, cells were pre-extracted in 10 mM Pipes pH 7.4, 100 mM NaCl, 300 mM sucrose and 3 mM $MgCl_2$ (CSK buffer) containing 0.5% (v/v) Triton X-100, for 5 min prior to PFA fixation as above. Incubation with primary antibodies (diluted in blocking buffer) was for 1 h at room temperature or at 4°C overnight. After washes, coverslips were incubated with Alexa-Fluor-conjugated goat antibodies (Alexa Fluor 488, 568 and 647) (Life Technologies), for 1 h at room temperature. After three washes in TPBS, DNA was stained in a 5-min incubation with DAPI diluted in TPBS. After one additional wash coverslips were mounted using Mowiol (Calbiochem).

Fluorescence images were acquired using a digital Leica DFC 350 FX CCD camera mounted on a Zeiss Axioplan inverted microscope. Identical exposure times were applied for different images within the same experiment. Images were processed and quantitative measurements of fluorescence intensities were performed with ImageJ software. All the images shown are from representative cells and were pseudocoloured according to the approximate emission wavelength of the fluorophores.

Confocal images were acquired using a LEICA TCS-SP5-AOBS microscope with an oil immersion 63× HCX PL APO objective lens. The nuclei were outlined using DAPI staining as a template and copied to the appropriate fluorophore channel. Nuclei were then counted and measurements of the mean fluorescent intensity or number of foci were recorded. Background was determined in images from incubations without primary antibody and was subtracted so that only the 'true signal' was analysed with the Find maxima tool from the ImageJ software. For colocalisation analysis, at least five confocal *z*-planes acquired every 0.5 µm were analysed using LAS AF software (Leica).

Detection of incorporated thymidine analogues EdU and IdU. Cells were pulse-labeled with 10 µM EdU and/or 25 µM IdU for the indicated times and fixed in 4% PFA for 15 min. The presence of EdU was monitored using the Click-it EdU Alexa Fluor 488 or 647 imaging kit (Life Technologies) according to the manufacturer's instructions. IdU staining was carried out after 15 min fixation in 4% PFA, followed by permeabilisation in 0.5% (v/v) Triton X-100 and DNA denaturation with 2 M HCl for 20 min. In IdU-EdU pulse-chase experiments, IdU staining preceded EdU detection. Coverslips were mounted as above.

EdU incorporation by flow cytometry

Cells were pulse labelled *in vivo* with 10 µM EdU for 10 min, fixed with 70% EtOH and kept overnight at −20°C. Next day, cells were washed three times in PBS and EdU incorporation into DNA labelled using the Click-it EdU Alexa Fluor 647 flow cytometry kit followed by propidium iodide (5 µg/ml) staining of total DNA. Cells were then analysed using a FACS Canto cytometer (Becton Dickinson) and analysed using FlowLogic software (Inivai Technologies).

Apoptosis assays

Apoptotic cells were scored using Annexin-V–FITC apoptotis detection kit (Bender MedSystems). Cultures 48 h after EtOH/4′OHT treatment were tripsinised, washed once in PBS followed by a wash 1× binding buffer. Then cells (1×10^6/ml, 0.1 ml) in binding buffer containing 5 µl of FITC-conjugated Annexin V and incubated 10 min at room temperature. After washes, 5 µl of PI staining solution were added and cells were acquired using a FACS Canto cytomer (Becton Dickinson) and analyzed using FlowLogic software (Inivai Technologies). Apoptosis was also assessed by conventional immunofluorescence (as above) using an anti-active caspase 3 (Promega).

DNA combing analysis

Replication analysis by DNA combing (Michalet et al., 1997) was performed as previously described (Domínguez-Sánchez et al., 2011). Briefly, 48 h after treatment, MEFs were pulsed with thymidine analogues IdU (25 µM) and CldU (200 µM) for the indicated times in each chase. Agarose plugs were prepared with 4×10^4 labelled cells per plug, and DNA fibres were extracted immediately after CldU labelling and stretched on silanised coverslips. DNA molecules were counterstained with an antibody against single-stranded DNA (MAB3034, Chemicon; 1:500) and an anti-mouse-IgG coupled to Alexa Fluor 546 (A11030, Molecular Probes, 1:50). CldU and IdU were detected with BU1/75 (AbCys, 1:20) and BD44 (Becton Dickinson, 1:20) anti-bromodeoxiuridina (BrdU) antibodies, respectively. DNA fibres were analysed on a Leica DM6000 microscope equipped with a DFC390 camera (Leica). Data acquisition was performed with LAS AF software (Leica).

Chromatin immunoprecipitation and qRT-PCR

Cross-linking of chromatin was performed by incubating cells in 1% formaldehyde for 15 min at room temperature. Residual aldehyde was quenched with glycine 0.125 M. After 3 washes with PBS, cells were scraped and resuspended in LB1 buffer (50 mM Hepes pH 7.4, 140 mM NaCl, 1 mM EDTA, 10% glycerol, 0.5% Igepal CA-630, 0.25% Triton X-100). After 5 min incubation in LB1 buffer, cells were centrifuged at 1350 ***g*** for 5 min, and pellets were resuspended in LB2 buffer (10 mM Tris-HCl pH 8, 200 mM NaCl, 1 mM EDTA, 0.5 mM EGTA), incubated for 5 min at 4°C and centrifuged for 5 min at 1350 ***g***. Pellets were resuspended in LB3 buffer (10 mM Tris-HCl pH 8.0 100 mM NaCl, 1 mM EDTA, 0.1% deoxycholate, 0.5% laurylsarcosine) and after 25 min incubation at 4°C, were sonicated for four 30-s cycles on the high intensity setting (Bioruptor, Diagenode). The sonicated lysates were centrifuged at 10,000 ***g*** for 10 min. Soluble chromatin (100–200 µg) was incubated with the indicated antibodies overnight at 4°C. Then, immunocomplexes were recovered with 15 µl of a suspension of paramagnetic protein G beads (Life Technologies), preblocked with 0.5% BSA (w/v) in PBS, during 2 h at 4°C on a rotating wheel. The immunoprecipitated chromatin was washed two times in low-salt buffer (20 mM Tris-HCl pH 8.1, 150 mM NaCl, 2 mM EDTA, 1% Triton X-100, 0.1% SDS), once in high-salt buffer (20 mM Tris-HCl pH 8.1, 500 mM NaCl, 2 mM EDTA, 1% Triton X-100, 0.1% SDS) and another time in LiCl buffer (10 mM Tris-HCl pH 8.1, 250 mM LiCl, 1 mM EDTA, 1% deoxycholate, 1% NP-40). Beads were incubated for 5 min at 100°C in 50 mM Tris-HCl pH 8.1, 10 mM EDTA, 1% SDS, and the eluted chromatin was treated overnight in 200 mM NaCl at 65°C. After RNAse and proteinase K treatment, DNA was purified by phenol-chloroform extraction and precipitated with EtOH for use in qRT-PCR) with primers spanning major satellite sequences (Pinheiro et al., 2012), forward, 5′-TGGAATATGGCGAGAAAACTG-3′ and reverse, 5′-AGGTCCTTCAGTGGGCATTT-3′; *Cdkn1a* sequences (Lüdtke et al., 2013), forward, 5′-GGCTTAGATTCCCAGAGGG-3′ and reverse, 5′-TTCTGGGGACACCCACTGG-3′; or *Actb* as a negative control, forward, 5′-GCAGGCCTAGTAACCGAGACA-3′ and reverse, 5′-AGTTTTGGC GATGGGTGCT-3′. All samples were normalised to unmodified core histone H2A sequence for each sample and enrichment is shown relative to mock DNA sample (only beads) using the same amount of DNA in the PCR.

Quantitative mRNA analysis

Major satellite transcripts were quantified by qRT-PCR. Total RNA was isolated using TRI Reagent solution (Sigma-Aldrich) according to the provided protocol. The RNA was reversed transcribed using a SuperScript VILO cDNA synthesis system (Life Technologies). qRT-PCR used the primers spanning major satellite repeats indicated above, and the data was analysed by the efficiency correction method (Pfaffl, 2001) using *Actb*, forward, 5′-GGCTGTATTCCCCTCCATCG-3′ and reverse, 5′-GGCTG-TATTCCCCTCCATCG-3′ as a normalising transcript.

Antibodies

Rabbit polyclonal anti-53BP1 antibody was from Novus Biological. Mouse monoclonal antibody (mAb) against Histone γH2Ax (2F3) was obtained from Biolegend and rabbit antibody against histone H3K9me3 was from Diagenode. Rat mAb anti-RPA32 (4E4), rabbit mAb anti-histone H2AK119Ub1 (D2754) and anti-histone H3K27me3 (C36B11) antibodies were acquired from Cell Signaling. Mouse anti-BrdU antibody (clone B44) for IdU detection was from Becton Dickinson. Anti-tubulin and anti-FLAG antibody M2 were from Sigma. Rabbit anti-histone H2A antibody was from Millipore. Anti-CDKN2A/p16^{Ink4a} (M-156) and CDKN1A/p21 (F-5) antibodies were acquired from Santa Cruz Biotechnology. Anti-RING1A and anti-RING1B antibodies were as described previously (García et al., 1999; Schoorlemmer et al., 1997).

Western blotting

Total cell extracts were prepared from cell lysates in RIPA buffer [10 mM Tris-HCl pH 7.2, 150 mM NaCl, 1% (v/v) Triton X-100, 0.1% SDS, 1% sodium deoxycholate and 5 mM EDTA] supplemented with 20 mM NaF and protease inhibitors (Complete, Roche). For histone extracts, cells were lysed in PBS containing 0.5% (v/v) Triton X-100, 2 mM PMSF, 4 mM N-ethyl-maleimide, and the nuclei were recovered, incubated overnight in 0.2 M HCl at 4°C and histones recovered in the soluble fraction. Proteins were separated by 10 or 15% SDS-PAGE and transferred onto nitrocellulose membranes. After blocking in 5% non-fat dry milk in PBS with 0.1% Tween 20 (TTBS), the membranes were incubated with primary antibodies, diluted in TTBS with 1% BSA for 1–2 h at room temperature or overnight at 4°C. Following TTBS washes, the membranes were incubated with horseradish-peroxidase-conjugated secondary antibodies (Dako) for 1 h at room temperature and luminescence detection using ECL Prime western blotting detection reagent (GE Healthcare).

Statistical analysis

Data were processed in Prism 6 (GraphPad software) using an unpaired, two-tailed Student's *t*-test, or Mann–Whitney U test, as indicated.

Acknowledgements

We are grateful to A. Berns (The Netherlands Cancer Institute, Amsterdam) for *Cdkn2ab* mutant mice, to S. Cooper (Oxford University, Oxford) for cDNAs encoding MBD1 fusion proteins and S. Temple (Neural Stem Cell Institute, New York) for plasmid expressing *Cdkn1a*/*p21* shRNA.

Competing interests

The authors declare no competing or financial interests.

Author contributions

M.B. carried out most experiments with contributions from F.N. and K.S.; S.B. performed combing experiments. M.B., C.C., A.A. and M.V. analysed the data. M.V. wrote the paper with input from M.B., C.C. and A.A.

Funding

This work was supported by the Ministerio de Economía y Competitividad (MINECO) [grant numbers BFU2010-18146, SAF2013-47997 to M.V.]; the CAM OncoCycle Programme [grant number S2010/BMD-2470 to M.V.]; and by a MINECO grant to A.A. [grant number BFU2013-42918-P]. M.B. and F.N. are recipients of MINECO and Campus de Excelencia Internacional Universidad Autónoma de Madrid + Consejo SUperior de Investigaciones Científicas (CEI UAM-CSIC) fellowships, respectively; K.S. is supported by FP7-PEOPLE-2011-ITN [grant number 289611].

Supplementary material

Supplementary material available online at
http://jcs.biologists.org/lookup/suppl/doi:10.1242/jcs.173021/-/DC1

References

Alabert, C. and Groth, A. (2012). Chromatin replication and epigenome maintenance. *Nat. Rev. Mol. Cell Biol.* **13**, 153-167.

Alabert, C., Bukowski-Wills, J.-C., Lee, S.-B., Kustatscher, G., Nakamura, K., de Lima Alves, F., Menard, P., Mejlvang, J., Rappsilber, J. and Groth, A. (2014). Nascent chromatin capture proteomics determines chromatin dynamics during DNA replication and identifies unknown fork components. *Nat. Cell Biol.* **16**, 281-293.

Alchanati, I., Teicher, C., Cohen, G., Shemesh, V., Barr, H. M., Nakache, P., Ben-Avraham, D., Idelevich, A., Angel, I., Livnah, N. et al. (2009). The E3 ubiquitin-ligase Bmi1/Ring1A controls the proteasomal degradation of Top2rocleavage complex – a potentially new drug target. *PLoS ONE* **4**, e8104-e8113.

Balajee, A. S. and Geard, C. R. (2004). Replication protein A and gamma-H2AX foci assembly is triggered by cellular response to DNA double-strand breaks. *Exp. Cell Res.* **300**, 320-334.

Bartkova, J., Rezaei, N., Liontos, M., Karakaidos, P., Kletsas, D., Issaeva, N., Vassiliou, L.-V. F., Kolettas, E., Niforou, K., Zoumpourlis, V. C. et al. (2006). Oncogene-induced senescence is part of the tumorigenesis barrier imposed by DNA damage checkpoints. *Nature* **444**, 633-637.

Bentley, M. L., Corn, J. E., Dong, K. C., Phung, Q., Cheung, T. K. and Cochran, A. G. (2011). Recognition of UbcH5c and the nucleosome by the Bmi1/Ring1b ubiquitin ligase complex. *EMBO J.* **30**, 3285-3297.

Bergink, S., Salomons, F. A., Hoogstraten, D., Groothuis, T. A. M., de Waard, H., Wu, J., Yuan, L., Citterio, E., Houtsmuller, A. B., Neefjes, J. et al. (2006). DNA damage triggers nucleotide excision repair-dependent monoubiquitylation of histone H2A. *Genes Dev.* **20**, 1343-1352.

Boyarchuk, E., Filipescu, D., Vassias, I., Cantaloube, S. and Almouzni, G. (2014). The histone variant composition of centromeres is controlled by the pericentric heterochromatin state during the cell cycle. *J. Cell Sci.* **127**, 3347-3359.

Bracken, A. P., Kleine-Kohlbrecher, D., Dietrich, N., Pasini, D., Gargiulo, G., Beekman, C., Theilgaard-Mönch, K., Minucci, S., Porse, B. T., Marine, J.-C. et al. (2007). The Polycomb group proteins bind throughout the INK4A-ARF locus and are disassociated in senescent cells. *Genes Dev.* **21**, 525-530.

Branzei, D. and Foiani, M. (2010). Maintaining genome stability at the replication fork. *Nat. Rev. Mol. Cell Biol.* **11**, 208-219.

Buchwald, G., van der Stoop, P., Weichenrieder, O., Perrakis, A., van Lohuizen, M. and Sixma, T. K. (2006). Structure and E3-ligase activity of the Ring–Ring complex of polycomb proteins Bmi1 and Ring1b. *EMBO J.* **25**, 2465-2474.

Bulut-Karslioglu, A., Perrera, V., Scaranaro, M., de la Rosa-Velazquez, I. A., van de Nobelen, S., Shukeir, N., Popow, J., Gerle, B., Opravil, S., Pagani, M. et al. (2012). A transcription factor601144teins Bmi1 and Ring1borkA-ARF locus and are di. *Nat. Struct. Mol. Biol.* **19**, 1023-1030.

Buonomo, S. B. C., Wu, Y., Ferguson, D. and de Lange, T. (2009). Mammalian Rif1 contributes to replication stress survival and homology-directed repair. *J. Cell Biol.* **187**, 385-398.

Calés, C., Román-Trufero, M., Pavón, L., Serrano, I., Melgar, T., Endoh, M., Pérez, C., Koseki, H. and Vidal, M. (2008). Inactivation of the polycomb group protein Ring1B unveils an antiproliferative role in hematopoietic cell expansion and cooperation with tumorigenesis associated with Ink4a deletion. *Mol. Cell. Biol.* **28**, 1018-1028.

Cao, R., Tsukada, Y.-i. and Zhang, Y. (2005). Role of Bmi-1 and Ring1A in H2A ubiquitylation and Hox gene silencing. *Mol. Cell* **20**, 845-854.

Chou, D. M., Adamson, B., Dephoure, N. E., Tan, X., Nottke, A. C., Hurov, K. E., Gygi, S. P., Colaiácovo, M. P. and Elledge, S. J. (2010). A chromatin localization screen reveals poly (ADP ribose)-regulated recruitment of the repressive polycomb and NuRD complexes to sites of DNA damage. *Proc. Natl. Acad. Sci. USA* **107**, 18475-18480.

Cimprich, K. A. and Cortez, D. (2008). ATR: an essential regulator of genome integrity. *Nat. Rev. Mol. Cell Biol.* **9**, 616-627.

Collins, N., Poot, R. A., Kukimoto, I., García-Jiménez, C., Dellaire, G. and Varga-Weisz, P. D. (2002). An ACF1eisznezm2450egulator of genome integrityDP ribose)-regulated recruitment of the repressive. *Nat. Genet.* **32**, 627-632.

Cooper, S., Dienstbier, M., Hassan, R., Schermelleh, L., Sharif, J., Blackledge, N. P., De Marco, V., Elderkin, S., Koseki, H., Klose, R. et al. (2014). Targeting polycomb to pericentric heterochromatin in embryonic stem cells reveals a role for H2AK119u1 in PRC2 recruitment. *Cell Rep.* **7**, 1456-1470.

de Napoles, M., Mermoud, J. E., Wakao, R., Tang, Y. A., Endoh, M., Appanah, R., Nesterova, T. B., Silva, J., Otte, A. P. and Vidal, M. (2004). Polycomb group proteins Ring1A/B link ubiquitylation of histone H2A to heritable gene silencing and X inactivation. *Dev. Cell* **7**, 663-676.

del Mar Lorente, M., Marcos-Gutiérrez, C., Pérez, C., Schoorlemmer, J., Ramírez, A., Magin, T. and Vidal, M. (2000). Loss- and gain-of-function mutations show a polycomb group function for Ring1A in mice. *Development* **127**, 5093-5100.

Di Croce, L. and Helin, K. (2013). Transcriptional regulation by Polycomb group proteins. *Nat. Struct. Mol. Biol.* **20**, 1147-1155.

Di Micco, R., Fumagalli, M., Cicalese, A., Piccinin, S., Gasparini, P., Luise, C., Schurra, C., Garre', M., Giovanni Nuciforo, P., Bensimon, A. et al. (2006). Oncogene-induced senescence is a DNA damage response triggered by DNA hyper-replication. *Nature* **444**, 638-642.

Domínguez-Sánchez, M. S., Barroso, S., Gómez-González, B., Luna, R. and Aguilera, A. (2011). Genome instability and transcription elongation impairment in human cells depleted of THO/TREX. *PLoS Genet.* **7**, e1002386.

Endoh, M., Endo, T. A., Endoh, T., Isono, K.-i., Sharif, J., Ohara, O., Toyoda, T., Ito, T., Eskeland, R., Bickmore, W. A. et al. (2012). Histone H2A mono-ubiquitination is a crucial step to mediate PRC1-dependent repression of developmental genes to maintain ES cell identity. *PLoS Genet.* **8**, e1002774.

Eskeland, R., Leeb, M., Grimes, G. R., Kress, C., Boyle, S., Sproul, D., Gilbert, N., Fan, Y., Skoultchi, A. I., Wutz, A. et al. (2010). Ring1B compacts chromatin structure and represses gene expression independent of histone ubiquitination. *Mol. Cell* **38**, 452-464.

Fasano, C. A., Dimos, J. T., Ivanova, N. B., Lowry, N., Lemischka, I. R. and Temple, S. (2007). shRNA knockdown of Bmi-1 reveals a critical role for p21-Rb pathway in NSC self-renewal during development. *Cell Stem Cell* **1**, 87-99.

Gao, Z., Zhang, J., Bonasio, R., Strino, F., Sawai, A., Parisi, F., Kluger, Y. and Reinberg, D. (2012). PCGF homologs, CBX proteins, and RYBP define functionally distinct PRC1 family complexes. *Mol. Cell* **45**, 344-356.

García, E., Marcos-Gutiérrez, C., del Mar Lorente, M., Moreno, J. C. and Vidal, M. (1999). RYBP, a new repressor protein that interacts with components of the mammalian Polycomb complex, and with the transcription factor YY1. *EMBO J.* **18**, 3404-3418.

Journal of Cell Science

Ginjala, V., Nacerddine, K., Kulkarni, A., Oza, J., Hill, S. J., Yao, M., Citterio, E., van Lohuizen, M. and Ganesan, S. (2011). BMI1 is recruited to DNA breaks and contributes to DNA damage-induced H2A ubiquitination and repair. *Mol. Cell. Biol.* **31**, 1972-1982.

Groth, A., Corpet, A., Cook, A. J. L., Roche, D., Bartek, J., Lukas, J. and Almouzni, G. (2007). Regulation of replication fork progression through histone supply and demand. *Science* **318**, 1928-1931.

Guenatri, M., Bailly, D., Maison, C. and Geneviève, A. (2004). Mouse centric and pericentric satellite repeats form distinct functional heterochromatin. *J. Cell Biol.* **166**, 493-505.

Helmrich, A., Ballarino, M., Nudler, E. and Tora, L. (2013). Transcription-replication encounters, consequences and genomic instability. *Nat. Struct. Mol. Biol.* **20**, 412-418.

Ismail, I. H., Andrin, C., McDonald, D. and Hendzel, M. J. (2010). BMI1-mediated histone ubiquitylation promotes DNA double-strand break repair. *J. Cell Biol.* **191**, 45-60.

Isono, K., Endo, T. A., Ku, M., Yamada, D., Suzuki, R., Sharif, J., Ishikura, T., Toyoda, T., Bernstein, B. E. and Koseki, H. (2013). SAM domain polymerization links subnuclear clustering of PRC1 to gene silencing. *Dev. Cell* **26**, 565-577.

Jasencakova, Z., Scharf, A. N. D., Ask, K., Corpet, A., Imhof, A., Almouzni, G. and Groth, A. (2010). Replication stress interferes with histone recycling and predeposition marking of new histones. *Mol. Cell* **37**, 736-743.

Kalb, R., Latwiel, S., Baymaz, H. I., Jansen, P. W. T. C., Müller, C. W., Vermeulen, M. and Müller, J. (2014a). Histone H2A monoubiquitination promotes histone H3 methylation in Polycomb repression. *Nat. Struct. Mol. Biol.* **21**, 569-571.

Kalb, R., Mallery, D. L., Larkin, C., Huang, J. T. J. and Hiom, K. (2014b). BRCA1 Is a Histone-H2A-Specific Ubiquitin Ligase. *Cell Rep.* **8**, 999-1005.

Klose, R. J., Cooper, S., Farcas, A. M., Blackledge, N. P. and Brockdorff, N. (2013). Chromatin samplingep.2014.07.025Ubiquitin Ligasergeting polycomb repressor proteins. *PLoS Genet.* **9**, e1003717.

Krimpenfort, P., IJpenberg, A., Song, J.-Y., van der Valk, M., Nawijn, M., Zevenhoven, J. and Berns, A. (2007). p15Ink4b is a critical tumour suppressor in the absence of p16Ink4a. *Nature* **448**, 943-946.

Lambert, S. and Carr, A. M. (2013). Impediments to replication fork movement: stabilisation, reactivation and genome instability. *Chromosoma* **122**, 33-45.

Lanzuolo, C. and Orlando, V. (2012). Memories from the polycomb group proteins. *Annu. Rev. Genet.* **46**, 561-589.

Lee, H.-S., Lee, S.-A., Hur, S.-K., Seo, J.-W. and Kwon, J. (2014). Stabilization and targeting of INO80 to replication forks by BAP1 during normal DNA synthesis. *Nat. Commun.* **5**, 5128.

Lu, J. and Gilbert, D. M. (2007). Proliferation-dependent and cell cycle regulated transcription of mouse pericentric heterochromatin. *J. Cell Biol.* **179**, 411-421.

Lüdtke, T. H.-W., Farin, H. F., Rudat, C., Schuster-Gossler, K., Petry, M., Barnett, P., Christoffels, V. M. and Kispert, A. (2013). Tbx2 controls lung growth by direct repression of the cell cycle inhibitor genes Cdkn1a and Cdkn1b. *PLoS Genet.* **9**, e1003189.

Lukas, J., Lukas, C. and Bartek, J. (2011). More than just a focus: the chromatin response to DNA damage and its role in genome integrity maintenance. *Nat. Cell Biol.* **13**, 1161-1169.

Maertens, G. N., El Messaoudi-Aubert, S., Elderkin, S., Hiom, K. and Peters, G. (2010). Ubiquitin-specific proteases 7 and 11 modulate Polycomb regulation of the INK4a tumour suppressor. *EMBO J.* **29**, 2553-2565.

McGinty, R. K., Henrici, R. C. and Tan, S. (2014). Crystal structure of the PRC1 ubiquitylation module bound to the nucleosome. *Nature* **514**, 591-596.

Mejlvang, J., Feng, Y., Alabert, C., Neelsen, K. J., Jasencakova, Z., Zhao, X., Lees, M., Sandelin, A., Pasero, P., Lopes, M. et al. (2014). New histone supply regulates replication fork speed and PCNA unloading. *J. Cell Biol.* **204**, 29-43.

Michalet, X., Ekong, R., Fougerousse, F., Rousseaux, S., Schurra, C., Hornigold, N., van Slegtenhorst, M., Wolfe, J., Povey, S., Beckmann, J. S. et al. (1997). Dynamic molecular combing: stretching the whole human genome for high-resolution studies. *Science* **277**, 1518-1523.

Nishiyama, A., Yamaguchi, L., Sharif, J., Johmura, Y., Kawamura, T., Nakanishi, K., Shimamura, S., Arita, K., Kodama, T., Ishikawa, F. et al. (2013). Uhrf1-dependent H3K23 ubiquitylation couples maintenance DNA methylation and replication. *Nature* **502**, 249-253.

Pan, M.-R., Peng, G., Hung, W.-C. and Lin, S.-Y. (2011). Monoubiquitination of H2AX protein regulates DNA damage response signaling. *J. Biol. Chem.* **286**, 28599-28607.

Papait, R., Pistore, C., Negri, D., Pecoraro, D., Cantarini, L. and Bonapace, I. M. (2007). Np95 is implicated in pericentromeric heterochromatin replication and in major satellite silencing. *Mol. Biol. Cell* **18**, 1098-1106.

Petruk, S., Black, K. L., Kovermann, S. K., Brock, H. W. and Mazo, A. (2013). Stepwise histone modifications are mediated by multiple enzymes that rapidly associate with nascent DNA during replication. *Nat. Commun.* **4**, 4841.

Pfaffl, M. W. (2001). A new mathematical model for relative quantification in real-time RT-PCR. *Nucleic Acids Res.* **29**, e45.

Pinheiro, I., Margueron, R., Shukeir, N., Eisold, M., Fritzsch, C., Richter, F. M., Mittler, G., Genoud, C., Goyama, S., Kurokawa, M. et al. (2012). Prdm3 and Prdm16 are H3K9me1 methyltransferases required for mammalian heterochromatin integrity. *Cell* **150**, 948-960.

Piunti, A., Rossi, A., Cerutti, A., Albert, M., Jammula, S., Scelfo, A., Cedrone, L., Fragola, G., Olsson, L., Koseki, H. et al. (2014). Polycomb proteins control proliferation and transformation independently of cell cycle checkpoints by regulating DNA replication. *Nat. Commun.* **5**, 3649.

Posfai, E., Kunzmann, R., Brochard, V., Salvaing, J., Cabuy, E., Roloff, T. C., Liu, Z., Tardat, M., van Lohuizen, M., Vidal, M. et al. (2012). Polycomb function during oogenesis is required for mouse embryonic development. *Genes Dev.* **26**, 920-932.

Quivy, J.-P., Roche, D., Kirschner, D., Tagamim, H., Nakatani, Y. and Almouzni, G. (2004). A CAF-1 dependent pool of HP1 during heterochromatin duplication. *EMBO J.* **23**, 3516-3526.

Quivy, J.-P., Gérard, A., Cook, A. J. L., Roche, D. and Almouzni, G. (2008). The HP1i038/sj.emboj.76003621 during heterochromatin duplicationic developmentll cycle checkpoints by regulating DNA replicat. *Nat. Struct. Mol. Biol.* **15**, 972-979.

Román-Trufero, M., Méndez-Gómez, H. R., Pérez, C., Hijikata, A., Fujimura, Y.-i., Endo, T., Koseki, H., Vicario-Abejón, C. and Vidal, M. (2009). Maintenance of undifferentiated state and self-renewal of embryonic neural stem cells by Polycomb protein Ring1B. *Stem Cells* **27**, 1559-1570.

Saksouk, N., Barth, T. K., Ziegler-Birling, C., Olova, N., Nowak, A., Rey, E., Mateos-Langerak, J., Urbach, S., Reik, W., Torres-Padilla, M.-E. et al. (2014). Redundant mechanisms to form silent chromatin at pericentromeric regions rely on BEND3 and DNA methylation. *Mol. Cell* **56**, 580-594.

Schoorlemmer, J., Marcos-Gutiérrez, C., Were, F., Martínez, R., García, E., Satijn, D. P. E., Otte, A. P. and Vidal, M. (1997). Ring1A is a transcriptional repressor that interacts with the Polycomb-M33 protein and is expressed at rhombomere boundaries in the mouse hindbrain. *EMBO J.* **16**, 5930-5942.

Schuettengruber, B., Chourrout, D., Vervoort, M., Leblanc, B. and Cavalli, G. (2007). Genome regulation by polycomb and trithorax proteins. *Cell* **128**, 735-745.

Schwartz, Y. B. and Pirrotta, V. (2013). A new world of Polycombs: unexpected partnerships and emerging functions. *Nat. Rev. Genet.* **14**, 853-864.

Sharif, J., Muto, M., Takebayashi, S.-i., Suetake, I., Iwamatsu, A., Endo, T. A., Shinga, J., Mizutani-Koseki, Y., Toyoda, T., Okamura, K. et al. (2007). The SRA protein Np95 mediates epigenetic inheritance by recruiting Dnmt1 to methylated DNA. *Nature* **450**, 908-912.

Simon, J. A. and Kingston, R. E. (2013). Occupying chromatin: Polycomb mechanisms for getting to genomic targets, stopping transcriptional traffic, and staying put. *Mol. Cell* **49**, 808-824.

Sims, J. K. and Wade, P. A. (2011). Mi-2/NuRD complex function is required for normal S phase progression and assembly of pericentric heterochromatin. *Mol. Biol. Cell* **22**, 3094-3102.

Vassilev, A. P., Rasmussen, H. H., Christensen, E. I., Nielsen, S. and Celis, J. E. (1995). The levels of ubiquitinated histone H2A are highly upregulated in transformed human cells: partial colocalization of uH2A clusters and PCNA/cyclin foci in a fraction of cells in S-phase. *J. Cell Sci.* **108**, 1205-1215.

Vissers, J. H. A., van Lohuizen, M. and Citterio, E. (2012). The emerging role of Polycomb repressors in the response to DNA damage. *J. Cell. Sci.* **125**, 3939-3948.

Voncken, J. W., Roelen, B. A. J., Roefs, M., de Vries, S., Verhoeven, E., Marino, S., Deschamps, J. and van Lohuizen, M. (2003). Rnf2 (Ring1b) deficiency causes gastrulation arrest and cell cycle inhibition. *Proc. Natl. Acad. Sci. USA* **100**, 2468-2473.

Wang, B., Matsuoka, S., Carpenter, P. B. and Elledge, S. J. (2002). 53BP1, a mediator of the DNA damage checkpoint. *Science* **298**, 1435-1438.

Wang, H., Wang, L., Erdjument-Bromage, H., Vidal, M., Tempst, P., Jones, R. S. and Zhang, Y. (2004). Role of histone H2A ubiquitination in Polycomb silencing. *Nature* **431**, 873-878.

Wu, R., Singh, P. B. and Gilbert, D. M. (2006). Uncoupling global and fine-tuning replication timing determinants for mouse pericentric heterochromatin. *J. Cell Biol.* **174**, 185-194.

Wu, C.-Y., Kang, H.-Y., Yang, W.-L., Wu, J., Jeong, Y. S., Wang, J., Chan, C.-H., Lee, S.-W., Zhang, X., Lamothe, B. et al. (2011). Critical role of monoubiquitination of histone H2AX protein in histone H2AX phosphorylation and DNA damage response. *J. Biol. Chem.* **286**, 30806-30815.

Zhu, Q., Pao, G. M., Huynh, A. M., Suh, H., Tonnu, N., Nederlof, P. M., Gage, F. H. and Verma, I. M. (2011). BRCA1 tumour suppression occurs via heterochromatin-mediated silencing. *Nature* **477**, 179-184.

Zou, L. and Elledge, S. J. (2003). Sensing DNA damage through ATRIP recognition of RPA-ssDNA complexes. *Science* **300**, 1542-1548.